Structure and Phase Transition of $GdBO_3$

M. Ren, J. H. Lin,* Y. Dong, L. Q. Yang, and M. Z. Su

State Key Laboratory of Rare Earth Materials Chemistry and Applications, Department of Materials Chemistry, Peking University, Beijing 100871, P. R. China

L. P. You

Laboratory of Microscopy, Peking University, Beijing 100871, P. R. China

Received January 12, 1999. Revised Manuscript Received April 6, 1999

The crystal structure and a phase transition of gadolinium orthoborate, $GdBO_3$, were studied by electron diffraction and X-ray powder diffraction. $GdBO_3$ crystallizes in the vaterite structure (LT), in a rhombohedral space group $R32$ with the lattice constants of $a = 6.6357(2)$ Å and $c = 26.706(1)$ Å. The structure of the LT phase was derived from the hexagonal YBO_3 structure and refined using X-ray powder diffraction data. The structure consists of tetrahedral polyborate group $B_3O_9^{9-}$ and the gadolinium atoms, located respectively on the 3-fold screw axis and a general position. The material undergoes a first-order phase transition with a large thermal hysteresis. The high-temperature (HT) phase crystallizes in a calcite related structure with the lattice constants of $a = 4.1154(2)$ and $c = 8.592(1)$ Å, which consists of planer triangular borate group BO_3^{3-}. The observed large thermal hysteresis of the phase transition is mainly caused by a structural change of the borate group, from $B_3O_9^{9-}$ in the LT phase to BO_3^{3-} in the HT phase.

1. Introduction

Lanthanide orthoborates $LnBO_3$ (Ln = rare earth and yttrium) are an interesting class of inorganic compounds. These materials show high VUV (vacuum ultraviolet) transparency and exceptional optical damage thresholds and, moreover, the Eu^{3+}- and Tb^{3+}-doped $LnBO_3$ exhibits extraordinarily high luminescent efficiency under VUV excitation and, thus are considered to be attractive candidates as VUV luminescent materials used in the gas discharge panels. In the last couple of years considerable effort has been devoted to improve the performance of these materials.[1] A problem of these materials in application is the color purity. For the Eu^{3+}-doped $GdBO_3$, for example, the emission spectrum is composed of almost equal contributions from the $^5D_0-^7F_1$ (580 nm) and $^5D_0-^7F_2$ (613 nm) transitions, which give rise to an orange-red color instead of deep red. In terms of application, concentration of the main emission in the $^5D_0-^7F_2$ transition is required. It is known that the $^5D_0-^7F_2$ transition is hypersensitive to the symmetry of the crystal field. Therefore, improving the performance, as well as any sensible interpretation of the luminescent properties, requires a well-defined crystal structure of these compounds.

$LnBO_3$ is compositionally the simplest of the compounds in the $Ln_2O_3-B_2O_3$ systems. The crystal structure determination, however, was far more complicated. Although numerous efforts have been devoted to the structure determination of these compounds, there are still considerable controversies left. Levin et al.[2] reported the general trend of the crystal structure of rare earth orthoborates $LnBO_3$ and proposed that their structures are related to the three crystalline forms of $CaCO_3$, aragonite, vaterite, and calcite. The orthoborates of the light rare earths (La to Nd) exhibit the aragonite-type structure and those of the heavy rare earths (Sm to Yb) possess the vaterite-type structure. In another class, $InBO_3$, $LuBO_3$, and $ScBO_3$ were known to form in the calcite-type structure. Phase transitions of the aragonite-type orthoborates, such as $LaBO_3$ and $NdBO_3$, were observed, but were not reported for the other orthoborates (Gd to Yb).[2] The aragonite- and calcite-type orthoborates contain triangular BO_3^{3-} groups, which has been confirmed by both X-ray diffraction and spectroscopic studies.[2,3] For the vaterite-type compounds (Sm to Yb), Newnham et al.[4] proposed two possible structure models, a disordered hexagonal ($P6_3/mmc$) structure and an ordered hexagonal ($P6_3/mcm$) structure. Bradley et al.[5] described the structure using the $P\bar{6}c2$ space group. A common feature of these models is that the borate group was assumed to be in triangular geometry (BO_3^{3-}). Later IR, NMR, and Raman studies,[6] however, revealed that these compounds contain only

* To whom correspondence should be addressed: Professor Jianhua Lin, telephone (86010)62751715, fax (86010)62751708, e-mail jhlin@chemms.chem.pku.edu.cn.

(1) Veenis, A. W.; Bril, A. *Philips J. Res.* **1978**, *33*, 124.

(2) Levin, E. M.; Roth, R. S.; Martin, J. B. *Am. Mineral* **1961**, *46*, 1030.

(3) Antic-Fidancev, E.; Aride, J.; Chaminade, J.; Lemaitre-Blaise, M.; Porcher, P. *J. Solid State Chem.* **1992**, *97*, 74. Bohlhoff, R.; Bambauer, H. U.; Hoffman, W. *Z. Kristallogr.* **1971**, *133*, 386.

(4) Newnham, R. E.; Redman, M. J.; Santoro, R. P. *J. Am. Ceram. Soc.* **1963**, *46*, 253.

(5) Bradley, W. F.; Graf, D. L.; Roth, R. S. *Acta Crystallogr.* **1966**, *20*, 283.

(6) Laperches, J. P.; Tarte, P. *Spectrochim. Acta* **1966**, *22*, 1201. Denning, J. H.; Ross, S. D. *Spectrochim. Acta* **1972**, *28A*, 1775. Kriz, H. M.; Bray, P. J. *J. Chem. Phys.* **1969**, *51*, 3624.

10.1021/cm990022o CCC: $18.00
Published on Web 05/22/1999

the tetrahedral polyborate group of $B_3O_9^{9-}$. Very recently, Chadeyron et al.[9] reinvestigated the crystal structure of YBO_3 by using single-crystal techniques and found that the structure, indeed, contains the $B_3O_9^{9-}$ group. In their structure model, the boron position and one oxygen position are partially occupied ($^1/_3$). Physically, this implies a rotational distortion of the $B_3O_9^{9-}$ group in the structure. With regard to the large anion size, it is unlikely that the $B_3O_9^{9-}$ group is rotationally distorted in this solid-state structure. Nevertheless, the structure model they proposed provides a reasonable basis for the structure of the vaterite type.

To verify the crystallographic results, several meticulous analyses of the luminescence spectra of Eu^{3+} doped YBO_3 materials were carried with the view of monitoring the local symmetry of the rare earth atoms.[7,8] Holsä[7] reported two kinds of sites with D_{3d} and T symmetry of Eu^{3+} for the rare earth atoms in $LnBO_3$. Chadeyron et al.[8] proposed two intrinsic sites of C_3 symmetry in YBO_3. Because of the importance in application, it is highly desirable to satisfactorily solve this structure. In this paper, we report the crystal structure studies of $GdBO_3$ using electron diffraction and X-ray powder diffraction, as well as observation of the phase transition from the vaterite type to the calcite structure.

2. Experimental Section

Powder samples of $GdBO_3$ were prepared by heating a mixture of Gd_2O_3 (99.99%) and H_3BO_3 in a ratio of 1:2.05. The mixture was first heated at 500 °C for 2 h to decompose the boric acid and then at 1100 °C for 2 h. After the reaction was complete, the products were annealed at 500 °C for about 3−4 weeks to improve their crystalline integrity. The samples obtained are white powders, and the phase purity was examined by X-ray powder diffraction. The in situ high-temperature X-ray powder diffraction patterns were recorded on a Rigaku D/max 2000 diffractometer with Cu Kα radiation from a rotating anode. The temperature of the sample furnace was controlled by a temperature controller attached to the X-ray diffractometer, and the measured temperature range was between 25 and 1000 °C. The X-ray powder diffraction data used in the structure refinement were collected at room temperature and 700 °C in a slow mode (step = 0.02°, rate = 0.5°/min). The electron diffraction was carried out on a Hitachi H-9000 electron microscope, and the IR spectra were recorded on a Nicolet Magna 750 FT-IR spectrometer.

3. Results and Discussion

DTA curves of $GdBO_3$, shown in Figure 1, clearly indicate a possible phase transition with large thermal hysteresis. The transform from the LT phase to the HT phase occurs at about 836 °C and, the reverse transition occurs at a lower temperature (546 °C). Selected X-ray diffraction patterns recorded at different temperatures are shown in Figure 2, which confirms the different structures for the LT and HT phase. Because the transition temperature from the HT to the LT phase is quite low on cooling, the crystalline integrity of the LT phase is not satisfactory when a conventional cooling rate is used. All of the samples used in this study, therefore, were annealed at 500 °C for several weeks.

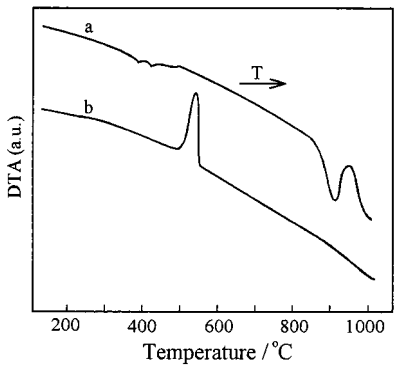

Figure 1. The differential thermal analysis curve of $GdBO_3$ on (a) heating and (b) cooling.

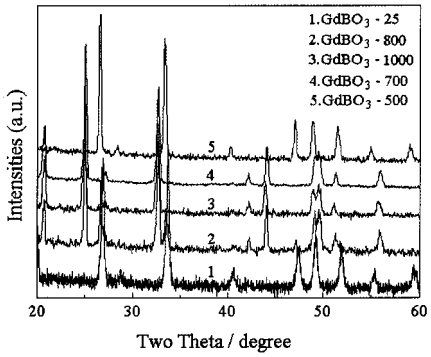

Figure 2. X-ray diffraction patterns of $GdBO_3$ at selected temperatures.

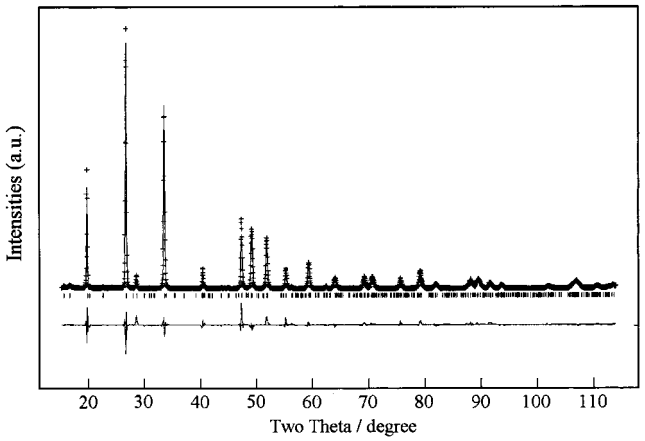

Figure 3. The Rietveld profile fits of diffraction data of the LT phase of $GdBO_3$. The symbols are the observed, background-subtracted intensities. The solid lines represent the calculated intensities. The tick marks indicate the positions of the Bragg reflections. Differences between the observed and calculated intensities are shown at the bottom of each panel.

Crystal Structure of LT Phase. The X-ray powder pattern of the LT phase of $GdBO_3$, shown in Figure 3, is very similar to that of YBO_3, so these two compounds crystallize in the same structure. In fact, the isomorphism of these two compounds is clearly evidenced from the IR spectra shown in Figure 4. The IR absorption peaks between 900 and 1050 cm^{-1} in YBO_3 and $GdBO_3$ are those typical for the tetrahedral borate group BO_4.[6] The typical absorption of a triangular BO_3 group appears, on the other hand, at about 1300 cm^{-1}, as in $LaBO_3$.[9]

(7) Holsä, J. *Inorg. Chim. Acta* **1987**, *139*, 257.
(8) Chadeyron, G.; Arbus, A.; Fournier, M. T.; Zambon, D.; Cousseins, J. C. *C. R. Acad. Sci. Ser. II* **1995**, *320b*, 199. Chadeyron, G.; Mahiou, R.; El-Ghozzi, M.; Arbus, A.; Zambon, D.; Cousseins, J. C. *J. Lumin.* **1997**, *72−74*, 564.
(9) Chadeyron, G.; El-Ghozzi, M.; Mahiou, R.; Arbus, A.; Cousseins, J. C. *J. Solid State Chem.* **1997**, *128*, 261.

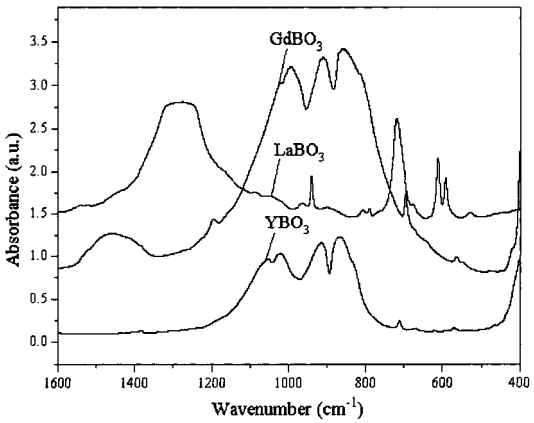

Figure 4. IR spectra of $LaBO_3$, YBO_3 and $GdBO_3$.

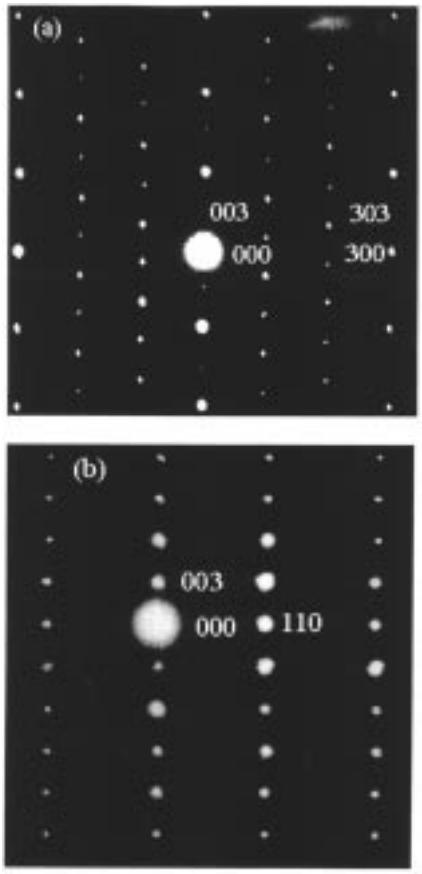

Figure 5. Electron diffraction patterns of $GdBO_3$ on (a) [010] and (b) [1$\bar{1}$0] directions.

Most of the reflections in $GdBO_3$ can be indexed by a hexagonal cell similar to that of YBO_3,[9] $a = 3.770$ Å and $c = 8.804$ Å. There are several very weak reflections, for example at $2\theta = 15.60$ and 16.61, which cannot be indexed with this hexagonal cell. To identify the correct unit cell, we decided to examine the electron diffraction of $GdBO_3$. Figure 5 shows the electron diffraction patterns in different orientations. The electron diffraction in Figure 5a shows a typical pattern for a rhombohedral structure in the [010] zone. The diffraction pattern in Figure 5b is of the [1$\bar{1}$0] zone. The rhombohedral lattice constants, derived from electron diffraction and refined from X-ray powder diffraction pattern, are $a = 6.6357(2)$ Å and $c = 26.706(1)$ Å. At this stage, it is clear that the hexagonal cell of YBO_3[9] is only a subcell of the rhombohedral structure, and that the weak superreflections were not observed in the single-crystal structure determination.[9] The relationship between the rhombohedral and the hexagonal cell can be expressed as $a_r = \sqrt{3}a_h$ and $c_r = 3c_h$. The reflection conditions observed from electron diffraction patterns are $-h + k + l = 3n$ for $hkil$ and $l = 3n$ for $000l$ and, the possible space groups of the LT phase are $R3$, $R\bar{3}$, $R32$, $R3m$ or $R\bar{3}m$.

Table 1. Selected Structure Parameters for LT and HT Phases of $GdBO_3$

	LT phase[a]				HT phase[b]		
	x	*y*	*z*		*x*	*y*	*z*
Gd	0.3358(3)	- 0.0014(2)	0.0820(2)	Gd	0	0	0
O1	- 0.009(2)	0.667(4)	0.120(6)	B	$^1/_3$	$^2/_3$	$^1/_4$
O2	0.021(4)	0.673(4)	0.049(7)	O	0.148(4)	0.296(4)	$^1/_4$
O3	0	0.214(6)	0				
O4	0	0.202(8)	$^1/_2$				
B1[c]	0.760	0	0				
B2[c]	0.760	0	$^1/_2$				

[a] Space group: $R32$. $a = 6.6357(2)$, $c = 26.706(1)$, $V = 1018.44(5)$. [b] Space group: $P6_3/mmc$. $a = 4.1154(2)$, $c = 8.592(1)$, $V = 126.03(2)$. [c] Not refined.

Although only part of the reflections were used in the single-crystal study, Chadeyron's structure model[9] is reasonable, as far as the yttrium position and the geometry of the polyborate $B_3O_9^{9-}$ are concerned. The partial occupation of one oxygen and the boron atoms in the hexagonal structure is a consequence of miss-assignment of the unit cell. Since the rhombohedral cell is nine times as large as the hexagonal cell, the polyborate $B_3O_9^{9-}$ groups can be arranged in a rhombohedral way to avoid the partial occupation of the oxygen and boron atoms. The atomic position of the yttrium atom in Chadeyron's structure model, which was transferred to a general position (18f, $x = {}^1/_3$, $y = 0$, and $z = {}^1/_{12}$), was used as a starting set for the structure determination. All of the possible space groups were employed for constructing the structure model, and only $R32$ led to a reasonable solution. The structure was refined by using the Rietveld technique[10] and the oxygen atoms were located on the difference Fourier map. The boron atoms cannot be identified from the refinement, because their scattering power is too small. They were inserted into the structure by considering the structure of the polyborate group $B_3O_9^{9-}$. The refinement leads to the residual value of $R_p = 0.12$ and $R_{wp} = 0.16$. In consideration of the large number of weak superreflections in such a large unit cell, this agreement is reasonable. In Figure 3, we show the Rietveld profiles of the X-ray powder pattern. The atomic parameters are listed in Table 1.

Figure 6 shows a view of the rhombohedral structure of $GdBO_3$. Unlike Chadeyron's model,[9] the $B_3O_9^{9-}$ groups are located on a 3-fold screw axis, and in this way, the oxygen and boron atoms are no longer partially occupied. A simple approach to understand this structure is to stack $B_3O_9^{9-}$ sheets. Figure 7 shows a sheet composed of $B_3O_9^{9-}$ and gadolinium atoms. As can be seen in Figure 6, the sheets are stacked in a rhombohedral fashion, forming a three-dimensional structure.

(10) Larson, A. C.; von Dreele, R. B. Report LAUR 86-748; Los Alamos National Laboratory: Los Alamos, NM, 1985.

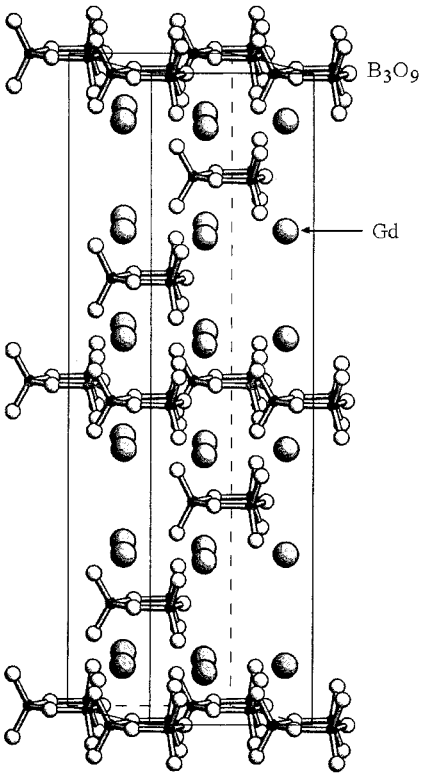

Figure 6. The crystal structure of the LT phase of $GdBO_3$.

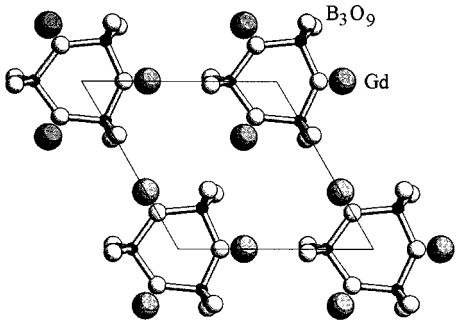

Figure 7. The $B_3O_9^{9-}$ sheet in the structure of LT phase of $GdBO_3$.

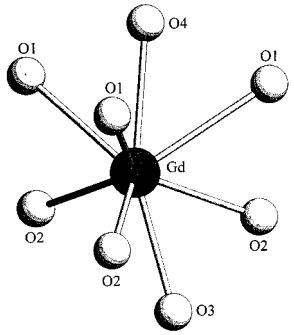

Figure 8. Coordination of gadolinium atom in LT phase of $GdBO_3$.

The gadolinium atoms in the structure are located on a general position with a bicapped trigonal prismatic coordination as shown in Figure 8. The capping oxygen atoms are above the triangular faces, but away from the pseudo-3-fold axis. The gadolinium atoms are in a C_1 symmetry coordination. For the Eu^{3+}-doped materials, the $^7F_1$ ground state splits into three levels and, three emission peaks of $^5D_0-^7F_1$ transition are expected.

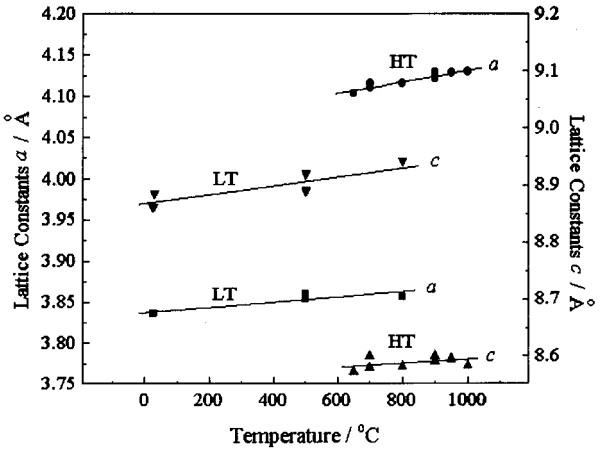

Figure 9. The temperature dependence of the lattice constants. All of the lattice constants are expressed in the hexagonal cell, i.e., $a = \sqrt{3}a_r$ and $c = c_r/3$.

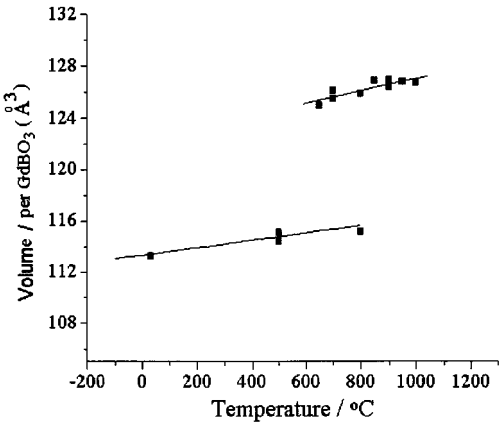

Figure 10. The temperature dependence of the unit-cell volume.

This is exactly what observed experimentally[8] in YBO_3:Eu^{3+}.

Phase Transition and Structure of the HT Phase. By taking advantage of the large thermal hysteresis of the phase transition, an X-ray diffraction pattern of HT phase was collected at 700 °C during the cooling process. The powder pattern of $GdBO_3$ was indexed by using the program TREOR in a package of PowderX.[11] The HT phase crystallizes in hexagonal space group $P63/mmc$ with the lattice constants of $a = 4.110(4)$ and $c = 8.579(4)$ Å at 700 °C. The lattice constants at other temperatures have also been calculated using the FINAX program. Figure 9 shows the variation of lattice constants with temperature. For comparison, the lattice constants of the LT phase are expressed using a hexagonal cell in the figure. It is seen that the lattice constants a and c are changing in different ways at the phase transition, i.e., the structure expands along the a axis and contracts along the c axis. Figure 10 shows the temperature dependence of the cell volume. The cell volume increases with temperature for both LT and HT phases due to the thermal expansion. A discontinuous change of the cell volume occurs between the two phases, indicating it is a first-order phase transition.

(11) Cheng, D. PowderX report; Institute of Physics, Chinese Academy of Sciences, 1997.

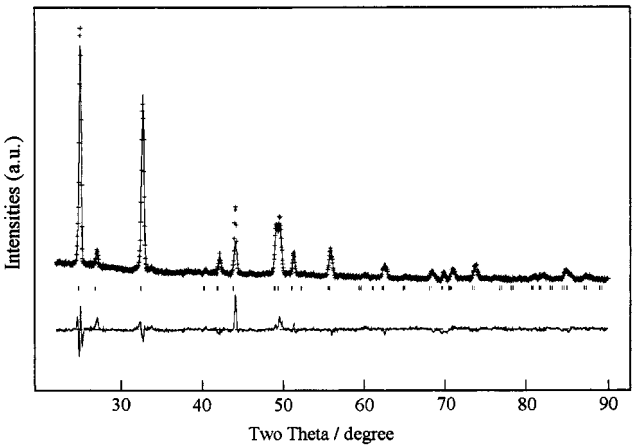

Figure 11. The Rietveld profile fits of diffraction data of the HT phase of $GdBO_3$ at 700 °C. The symbols are the observed, background-subtracted intensities. The solid lines represent the calculated intensities. The tick marks indicate the positions of the Bragg reflections. Differences between the observed and calculated intensities are shown at the bottom of each panel.

To establish the structure model of the HT phase, a full-pattern decomposition program EXTRA[12] was used to extract integrated intensities from the powder pattern. Thirty-one individual reflections, in which 26 are nonoverlapping reflections, were obtained. The crystal structure was solved with the direct method using the program SIRPOW.[13] The gadolinium atom position was recognized directly from the E map and was used as the starting point for the Rietveld refinement. The oxygen atom can be located during the refinement using a difference Fourier map. At this stage, it was clear that the crystal structure is related to the calcite type. The boron atom was, then, inserted into the structure by considering the structure of the BO_3^{3-} group. The structure was refined by the Rietveld procedure using the GSAS program,[10] and the residual values are $R_p = 0.031$ and $R_{wp} = 0.047$. The refined X-ray powder pattern is shown in Figure 11, and the atomic parameters are included in Table 1.

(12) Altomare, A.; Burla, M. C.; Cascarano, G.; Giacovazzo, C.; Guagliardi, A.; Moliterni, A. G. G.; Polidiori, G. *J. Appl. Crystallogr.* **1995**, *28*, 842.

(13) Altomare, A.; Cascarano, G.; Giacovazzo, C.; Guagliardi, A. SIRPOW user's manual; Inst. Di Ric. Per lo Sviluppo di Metodologie Cristallografiche, CNR.

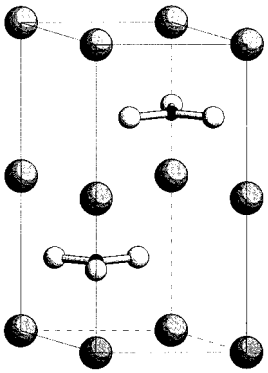

Figure 12. The crystal structure of the HT phase of $GdBO_3$.

Figure 12 shows the crystal structure of the HT phase. It is a simple structure, in which the planner triangular BO_3^{3-} groups are orientated perpendicular to the *c* axis, forming an anion sheet. It is this arrangement of the BO_3^{3-} groups, which causes the expansion of the *a* axis and the extraction of the *c* axis during the phase transition. The gadolinium atoms are located between the sheets and coordinated in a trigonal antiprismatic polyhedron. It is clear from these structure models that during the phase transition, the borate group changes from $B_3O_9^{9-}$ to BO_3^{3-}, while the gadolinium atoms almost remain at their positions. The rearrangement of the oxygen and boron atoms, as well as the B−O bond breakage and formation, should be the reason for the large thermal hysteresis of the phase transition.

In conclusion, by using electron and X-ray diffraction techniques, we have established crystal structure models for the LT and HT phases of $GdBO_3$. The LT phase crystallizes in a rhombohedral structure, containing $B_3O_9^{9-}$ groups. The gadolinium atoms are located in a general position with a bicapped trigonal prismatic coordination. The structure of the HT phase of $GdBO_3$ is related to the calcite type. The large thermal hysteresis of the phase transition is related to the structure change of the borate groups, from $B_3O_9^{9-}$ to BO_3^{3-}.

Acknowledgment. We are thankful to the financial support from the Youth Scientist Excellency Foundation (29625101), NSFC (29731010), Rhodia Rare Earth Co., and the State Key Basic Research Program.

CM990022O